Free Radical Research, February 2009; 43(2): 138–148

informa
healthcare

Oxidative-induced membrane damage in diabetes lymphocytes: Effects on intracellular Ca^{2+} homeostasis

SILVIA BELIA[1], FRANCESCA SANTILLI[1], SARA BECCAFICO[1,2], LUCREZIA DE FEUDIS[1], CATERINA MORABITO[1,2], GIOVANNI DAVÌ[1], GIORGIO FANÒ[1,2], & MARIA A. MARIGGIÒ[1,2]

[1]*Center of Excellence on Aging, G. D'Annunzio University Foundation, via Colle dell'Ara, I-66013 Chieti, Italy, and* [2]*Department of Basic and Applied Medical Sciences, University G. d'Annunzio of Chieti-Pescara, via dei Vestini 29 66013 Chieti, Italy*

(Received 28 September 2008; revised 27 October 2008)

Abstract
Oxidative stress is linked to several human diseases, including diabetes. However, the intracellular signal transduction pathways regulated by reactive oxygen species (ROS) remain to be established. Deleterious effects of ROS stem from interactions with various ion transport proteins such as ion channels and pumps, primarily altering Ca^{2+} homeostasis and inducing cell dysfunction. This study characterized the Ca^{2+} transport system in lymphocytes of patients with type-2 diabetes, evaluating the possible correlation between cell modifications and the existence of specific oxidative stress damage. Lymphocytes from type-2 diabetes patients displayed oxidative stress features (accumulation of some ROS species, membrane peroxidation, increase in protein carbonyls, increase in SOD and Catalase activity) and Ca^{2+} dyshomeostasis (modified voltage-dependent and inositol 1,4,5-triphosphate-mediated Ca^{2+} channel activities, decrease in Ca^{2+} pumps activity). The data support a correlation between oxidative damage and alterations in intracellular Ca^{2+} homeostasis, possibly due to modification of the ionic control in lymphocytes of type-2 diabetes patients.

Keywords: *Oxidative stress, calcium signaling, lymphocytes, calcium channels, ROS*

Introduction

The increasing global prevalence of diabetes mellitus (DM) is commonly associated with both microvascular and macrovascular complications. There is considerable evidence that hyperglycemia is the main cause of complications in DM and oxidative stress resulting from increased generation of reactive oxygen species (ROS) plays a crucial role in pathogenesis [1]. In the absence of the appropriate endogenous antioxidant mechanisms, redox imbalance activates stress-sensitive intracellular signalling pathways, which play a key role in the development of late complications of DM.

Hyperglycemia stimulates ROS production through several pathways, including redox imbalance secondary to increased aldose reductase (AR) activity and sorbitol accumulation via the polyol pathway, followed by advanced glycation end products (AGE) [2], altered protein kinase C (PKC) activity that further enhances hyperglycemia and tissue hypoxia, prostanoid imbalance and mitochondrial over-production of superoxide [3]. Hyperglycemia additionally leads to the glycation of antioxidant enzymes, which may alter their structure and function, rendering them unable to detoxify free radicals [4].

In DM, altered endothelium-dependent vascular relaxation is associated with hyperglycemia-derived

Correspondence: Professor Maria A. Mariggiò, Section of Physiology and Pathology of the Nervous System, Department of Basic and Applied Medical Sciences, 'G. d'Annunzio' University of Chieti-Pescara, via dei Vestini 31, 66013 Chieti, Italy. Tel: +39 0871 3554048. Fax: 0871 3554043. Email mariggio@unich.it

ISSN 1071-5762 print/ISSN 1029-2470 online
DOI: 10.1080/10715760802629588

oxygen free radicals [5]. AGEs activate the transcription factor, NF-kB, by enhancing intracellular oxidative stress, thus promoting the upregulation of various NF-kB-regulated target genes encoding cytokines and adhesive proteins and a switch to the prothrombotic phenotype of endothelial cells. Moreover, ROS enhance the sensitivity of contractile elements to Ca^{2+} and promote the mobilization of cytosolic Ca^{2+} in vascular smooth muscle cells [6]. Elevated lipid peroxidation may trigger increased thromboxane-dependent platelet activation in both type 1 and type 2 DM [7,8].

Calcium homeostasis is impaired in DM, which contributes to vascular complications [9,10]. The issue of whether defective Ca^{2+} metabolism precedes or succeeds the occurrence of diabetes is currently unclear. Intracellular calcium homeostasis, regulated by the redox status of cellular thiols and cell calcium concentration, may play a critical role in the control of a wide variety of cellular functions, including gene transcription and expression [9].

To evaluate whether the pathogenesis of DM is associated with increased levels of ROS, it is necessary to confirm the following events: (i) significant accumulation of ROS derived from lymphocyte cell metabolism, (ii) definite oxygen radical damage not seen in matched controls and (iii) abnormalities in the antioxidant defenses in diabetic patients. The validation of these conditions is essential to establish the possible relationship with cascade signalling events directly correlated with pathogenesis of the disease.

In this study, we characterize the cellular Ca^{2+} transport system of patients with type 2 diabetes in comparison to healthy individuals, with a view to evaluating the possible correlation between relevant modifications and the existence of specific oxidative stress damage sites. We employ lymphocytes as a model to study the pathophysiology of diabetes mellitus. These cells offer several advantages for cellular and molecular studies, such as easy accessibility, well characterized Ca^{2+} signalling pathways and conservation of the original phenotype after immortalization. Moreover, in lymphocytes, the Ca^{2+} transport mechanism resembles that in other muscular and non-muscular cells of patients affected by DM; hence, findings in lymphocytes may contribute to our understanding of effects in other cells.

Material and methods

Materials

All media, sera, antibiotics and culture solutions were purchased from Gibco BRL (Paisley, Scotland, UK). All sterile culture plastics were provided by Falcon (Plymouth, UK). All other reagents were analytical grade.

Patients

A total of 30 diabetic patients attending the Department of Internal Medicine, Pescara Civic Hospital, Italy, were examined on several occasions. All clinical investigations were conducted according to Declaration of Helsinki principles. Written consent was obtained from each participant. The local Ethics Committee approved the protocol used. Baseline characteristics of patients and healthy subjects are presented in Table I.

Isolation of human lymphocytes

Peripheral venous blood samples from healthy donors and DM patients were collected in sodium-heparinized vacutainers. Peripheral blood lymphocytes were separated under sterile conditions on a Ficoll-Paque PLUS (Amersham, Piscataway NY) gradient using the Boyum method [11]. Aliquots of heparinized whole blood diluted with an equal volume of Dulbecco's phosphate-buffered saline (1:1) were gently applied to an equal volume of Ficoll-Paque PLUS in centrifuge tubes. Samples were centrifuged at 400 xg for 30 min. The resultant interface (buffy coat) was carefully aspirated from the gradient and washed twice in Dulbecco's phosphate-buffered saline by centrifugation at 200 xg for 10 min. The subsequent pellet was resuspended in RPMI 1640 medium supplemented with 10% FBS, 2% L-glutamine, 1% penicillin/streptomycin. Monocytes were removed from the mononuclear fraction by adherence to Petri dishes during overnight incubation at 37°C. Purified lymphocytes were finally resuspended in complete RPMI 1640 medium ($1–2 \times 10^6$ cells/ml). Cell viability was determined by Trypan blue dye exclusion. The purified lymphocytes were used for experimental analyses within 2 days from their isolation.

ROS generation

Determination of hydrogen peroxide production. Hydrogen peroxide (H_2O_2) generation in lymphocytes from healthy and DM subjects was assayed using a colorimetric method involving the oxidation of iodide in the

Table I. Variables in diabetic patients (DM) and healthy controls (healthy).

		DM (30)	Healthy (29)
Age, years	mean±SD	65.2±12.7	57.4±16.5
Male gender	*n* (%)	22 (73,3)	12 (41.4)
Fasting plasma glucose (mg/dL)	mean±SD	176.2±83.3	86.8±19.3
HbA_{1c} (%)	mean±SD	8.4±2.1	/
Hypertension	*n* (%)	15 (50)	5 (17.2)
Hypercholesterolemia	*n* (%)	7 (23.3)	8 (27.6)
Hypertriglyceridemia	*n* (%)	3 (10)	2 (6.9)
ACE-I or ARB	*n* (%)	9 (30)	3 (10.3)
Statins	*n* (%)	3 (10)	1 (3.4)

presence of ammonium molybdate and photometric analyses of the resulting blue starch-iodine complex performed at 570 nm [12]. Briefly, human blood lymphocytes were treated with 38.5 mM HCl, 80 mM potassium iodide, 80 mM ammonium molybdate in H_2SO_4 and 0.38% starch. At 20 min after adding potassium iodide, sample absorbance was measured at 570 nm using a Titertek Multiskan MC plate reader (ICN/Flow Biochemicals, Huntsville, AL). The H_2O_2 concentration was estimated using a standard curve. Results are expressed as μg H_2O_2 per 10^5 cells.

Determination of $O_2^{\bullet -}$ release. Intracellular super oxide anion ($O_2^{\bullet -}$) production in lymphocytes from healthy and DM subjects was assayed as previously described [13], using a colorimetric method based on the reaction between Nitro Blue Tetrazolium (NBT) chloride and $O_2^{\bullet -}$, with the consequent formation of Formazan salt. Briefly, human blood lymphocytes were incubated with 1 mg/ml NBT at 37°C for 3 h. Next, cells were centrifuged (at 500 × g for 10 min) and the pellets treated with dimethyl sulphoxide (DMSO) at 37°C for 20 min. The absorbance of Formazan salt was measured at 550 nm using DMSO as the blank.

Oxidative damage

Protein carbonyl measurement. The protein carbonyl content was assayed by reacting 2,4-dinitrophenylhydrazine (DNPH) and protein carbonyls. DNPH reacts with protein carbonyls, forming a Schiff base to produce the corresponding hydrazone, which can be analysed spectrophotometrically [3]. We employed a protein carbonyl assay kit from Cayman Chemical (Ann Arbor, MI). Healthy and DM lymphocytes were rinsed with phosphate-buffered saline to remove red blood cells and sonicated in 10 volumes of buffer containing 50 mM MES, pH 6.7 and 1 mM EDTA. The sonicated cytosolic fraction was obtained by centrifugation at 10 000 xg for 15 min at 4°C. The supernatant protein concentration was set in the range of 1–10 mg/ml. We added 800 μl of DNPH or 800 μl of HCl (2.5 M) as the blank control to 200 μl protein. Samples and blanks were left at room temperature (RT) for 1 h in the dark and vortexed every 15 min. Trichloroacetic acid (TCA) was added (1 ml of 20%) to the samples. After incubation for 5 min on ice, samples and blanks were centrifuged at 10 000 × g for 10 min at 4°C. The resulting pellet was resuspended in 1 ml of 10% TCA and centrifuged at 10 000 × g for 10 min at 4°C. Next, the pellet was resuspended in 1 ml of ethanol/ethyl acetate mixture (1:1) and centrifuged at 10 000 × g for 10 min at 4°C. This step was repeated three times. After the final wash, protein pellets were resuspended in 500 μl of guanidine hydrochloride and centrifuged at 10 000 × g for 10 min at 4°C. The carbonyl content was determined based on supernatant absorbance at 370 nm, using a molar adsorption coefficient for DNPH of 22 000 $m^{-1}cm^{-1}$. Results are expressed as nmol of DNPH per mg of protein.

MDA measurement. Malondialdehyde (MDA) forms an adduct with thiobarbituric acid (TBA), which is measurable using a spectrophotometer. For lipid peroxidation analysis, we used the OXItek TBARS Assay Kit (ZeptoMetrix Corporation, Buffalo, NY). We mixed 100 μl of SDS and 100 μl of samples obtained from sonicated lymphocytes (in 9% NaCl) and then added 2.5 ml of TBA Buffer Reagent. Samples were incubated at 95°C for 1 h. The reaction was stopped by cooling in an ice bath for 10 min. After centrifugation at 3000 rpm for 15 min, the supernatant absorbance was read at 532 nm. The amount of MDA was calculated using a standard curve. Results are expressed as nmol of MDA per mg of protein [14].

Antioxidant enzyme activities

Antioxidant enzyme assays were performed using samples obtained from sonicated lymphocytes suspended in 20 mM Na-phosphate buffer, pH 7.0, along with 1 μg/ml pepstatin, 1 μg/ml leupeptin and 100 μM phenylmethylsulphonyl fluoride (PMSF) as protease inhibitors and centrifuged at 100 000 xg for 1 h at 4°C. Cytosol protein concentrations were measured according to the method of Lowry et al. [15].

Catalase activity was determined based on the decrease in absorbance due to H_2O_2 consumption ($\varepsilon = -0.04$ mM^{-1} cm^{-1}) measured at 240 nm, according to the method previously described [16]. The final reaction volume of 1 ml contained 100 mM Na-phosphate buffer, pH 7.0, 12 μM H_2O_2 and 70 μg of sample.

Glutathione S-transferase activity was determined according to a previously described procedure [17], using 1-chloro-2-4-dinitrobenzene (CDNB) as the substrate. The assay was performed at 340 nm ($\varepsilon =$ 9.6 mM^{-1} cm^{-1}) and the final reaction volume of 1 ml contained 100 mM Na-phosphate buffer, pH 6.5, 1 mM CDNB, 1 mM reduced glutathione (GSH) and 30 μg of sample.

Superoxide dismutase (SOD) activity was determined using the modified method of L'Abbé and Fischer [18]. The final assay volume (1 ml) contained 20 mM Na_2CO_3, pH 10, 10 μM cytochrome c, 1 mM xantine and xantine oxidase. As the xanthine oxidase activity varies, the amount used for the assay was sufficient to stimulate cytochrome c reduction at 550 nm at a rate of 0.025 per minute without SOD addition. SOD units were calculated on the basis of

the definition that one unit represents the activity that inhibits cytochrome c reduction by 50%.

Glutathione reductase (GR) activity was measured based on the decrease in absorbance induced by NADPH oxidation at 340 nm ($\varepsilon = -6.22$ mM^{-1} cm^{-1}) [19]. The assay mixture contained 100 mM Na-phosphate buffer, pH 7.0, 1 mM glutathione disulphide (GSSG), 60 μM NADPH and 100 μg of sample in a final volume of 1 ml.

Glutathione peroxidase activity was calculated using the method of Lawrence and Burk [20], which involves the measurement of GSSG formation using a coupled enzyme system with glutathione reductase. NADPH oxidation was recorded at 340 nm ($\varepsilon = -6.22$ mM^{-1} cm^{-1}). Selenium dependence was determined using H_2O_2 as the substrate. The final reaction volume of 1 ml contained 100 mM Na phosphate buffer, pH 7.5, 1 mM EDTA, 1 mM NaN_3, 2 mM GSH, 1 U GR, 0.24 mM NADPH, 30–80 μg sample and 0.6 mM H_2O_2.

Ca^{2+} homeostasis

Dihydropyridine receptor Ca^{2+} channel binding. The binding assay was performed on membranes purified after cell sonication (one pulse/s; 40 s) in Na phosphate buffer (20 mM, pH 7.0) supplemented with protease inhibitors as previously reported [21]. The dihydropyridine receptor (DHPR) concentration was determined using the radioligand [^{3}H]PN200-110. Proteins (40 μg) were incubated in a final volume of 250 ml binding buffer in the presence of 1 nM [^{3}H]PN200-110 for 1 h at RT. Then samples were filtered with Whatman GF/C filters and washed with six volumes of ice-cold washing buffer. Radioactivity was determined by liquid scintillation counting (LS 6500 Multi-Purpose Counter, Beckman Coulter, Fullerton, CA). Non-specific [^{3}H]PN200-110 binding was assessed in the presence of 10 μM unlabelled nifedipine and subtracted from each experimental point [22].

Ryanodine Ca^{2+} channel binding. This assay was performed on whole homogenates (25 μg of protein) obtained from sonicated lymphocytes [23]. Samples were incubated in 250 μl binding buffer solution containing 200 mM KCl, 10 mM HEPES, 100 μM $CaCl_2$, 0.1 mM DIFP and 1 μg/ml leupeptin, pH 7.4, in the presence of 5 nM [^{3}H]Ryanodine for 120 min at 37°C. Next, samples were filtered through Whatman GF/B filters and rinsed with six volumes of ice-cold 200 mM KCl, 10 mM HEPES, pH 7.4. The amount of bound [^{3}H]Ryanodine was determined by liquid scintillation counting using a LS 6500 Multi-Purpose Scintillation Counter (Beckman Coulter), and expressed as pmol per mg of protein. Non-specific binding was assessed in the presence of 100 μM unlabelled ryanodine and subtracted from each experimental point. However, none of the non-specific binding points was higher than 5–8% of total binding.

IP_3 Ca^{2+} channel binding. This assay was performed on whole homogenates obtained from sonicated lymphocytes [24]. The radioligand, [^{3}H] IP_3, was used for binding. Samples (200 μg of protein) were incubated in a final volume of 250 μl binding buffer solution containing 110 mM KCl, 20 mM NaCl, 1 mM Na_2HPO_4, 1 mM EDTA, 25 mM HEPES/KOH, 1 mM DTT, 0.1 mM diisopropylfluorophosphate (DIFP) and 1 μg/ml leupeptin, pH 7.4, in the presence of 1 nM [^{3}H]IP_3 for 6 min at 4°C. Membrane-bound [^{3}H]IP_3 was determined by filtration through Whatman GF/C filters, followed by rinsing of the filters with six volumes of ice-cold 250 mM sucrose, 10 mM Na_2HPO_4, pH 8.0. Radioactivity was determined by liquid scintillation counting using a LS 6500 Multi-Purpose Scintillation Counter (Beckman Coulter) and expressed as pmol per mg of protein.

Ca^{2+} pump activity. This assay was carried out on whole homogenates obtained from sonicated lymphocytes [25]. Each test tube contained 25 μg protein incubated with 2.5 mM ATP for 30 min at RT in 1 ml of mixture containing 100 μM $CaCl_2$, 60 μM K-EGTA, 10 mM KCl, 5 mM $MgCl_2$, 300 mM sucrose, 10 mM HEPES, pH 7.4. The reaction was terminated with 1 ml of 12.5% TCA and the precipitate removed by centrifugation at 5000 × g for 10 min. Released phosphates were estimated from 1 ml of clear supernatant, according to the method previously described [26]. Specific activity was calculated as μg of released P_i per min per ml per mg of protein.

Single cell Ca^{2+} video imaging. The intracellular calcium content was monitored using the calcium-sensitive fluorescent indicator, Fluo4/AM (Molecular Probes, Eugene, OR) and a Bio-Rad MRC-1024 ES confocal system (Bio-Rad Microscience Ltd, Hemel Hempstead, UK) connected to an inverted Zeiss Axiovert 100 microscope equipped with a 63 × /1.25 PLAN NEOFLUAR oil immersion objective (ZEISS, Jena, Germany) [27]. Isolated lymphocytes (300 000 cells/ml) were loaded in suspension with 3 μM Fluo4/AM for 30 min at 37°C in normal external solution (NES) containing 10 mM glucose, 140 mM NaCl, 2.8 mM KCl, 2 mM $CaCl_2$, 2 mM $MgCl_2$ and 10 mM HEPES, pH 7.4, supplemented with 1% BSA. Cells were centrifuged at 400 x*g* for 10 min and washed twice to remove extracellular dye. Next, cells were resuspended in NES, plated on poly-L-lysine-coated 12 mM glass coverslips set into an Attofluor chamber (Molecular Probes) and maintained for 5 min at RT to allow adhesion before image acquisition. Cells were incubated at RT during the experimental period and

usage of each coverslip did not exceed 15 min. Green fluorescence was recorded by setting excitation at 488 nm and emission at 522 nm using a bandpass filter (bandwidth $\pm$ 32 nm). Frames (256×256 pixels) were sampled every 2 s using a Kalman filter ($n = 2$), stored and analysed offline using LaserSharp 3.1 software (BioRad). Calibration of the Ca^{2+} transients was performed essentially using the method previously described [28]. Briefly, after recording cell fluorescence, lymphocytes were incubated with 1 μM ionomycin (a non-fluorescent ionophore) in NES solution and increased fluorescence of single Fluo4-loaded cells (F_{max}) was recorded within 1 min. Cells bathed with NES containing 6 mM EGTA (a Ca^{2+} chelator) displayed a sudden decrease in fluorescence and the fluorescence of single Fluo4-loaded cells (F_{min}) was recorded within 1 min. In each experiment, background fluorescence (F_{bkg}) was measured on a lymphocyte-free yield, while the cell autofluorescence value (F_{auto}) was calculated as the mean value of autofluorescence of 10 unloaded lymphocytes recorded on the same day. $[Ca^{2+}]_i$ was calculated using the following formula:

$$[Ca^{2+}]i = K_d \times[(F - F_{auto} - F_{bkg}) - F_{min}/F_{max} - (F - F_{auto} - F_{bkg})]$$

where K_d is the dissociation constant of calcium binding to Fluo4/AM (345 nm) and F is the fluorescence emission of a single Fluo4-loaded cell at times ranging from 2–x s.

For each experimental condition, at least five fields in different coverslips were analysed.

Statistical analysis

Statistical significance was calculated using the Student's t-test for unpaired data.

Results

Oxidative stress

Under our experimental conditions, increased levels of reactive oxygen species (H_2O_2 and $O_2^{\bullet -}$) were observed in isolated lymphocytes from DM patients, compared to controls. Specifically, H_2O_2 generation was higher in DM lymphocytes (1.87 ± 0.03 vs 0.99 ± 0.01, $p < 0.01$), while a small but significant increase in the concentration of $O_2^{\bullet -}$ was observed in diabetics, compared to healthy subjects (75.80 ± 0.37 vs 72.40 ± 0.60, $p < 0.01$) (Table II).

Considerable oxidative damage of membrane lipids, as reflected by MDA levels (12.43 ± 1.44 vs 7.83 ± 1.11, $p < 0.05$) and protein substrates, assessed from protein carbonyl levels (6.32 ± 0.15 vs 3.58 ± 0.24, $p < 0.01$), was observed in DM patients compared to controls. These data collectively indicate that the 'oxidative stress status' could derive from ROS over-production in lymphocytes from DM patients (Table II).

Specific activities of the main antioxidant enzymes are shown in Table II. Endogenous scavengers exhibited increased activity in DM samples, particularly superoxide dismutase (SOD), which transforms the superoxide anion radical into oxygen and hydrogen peroxide (42.50 ± 5.10 vs 97.00 ± 3.80; $p < 0.01$, controls vs DM samples). Moreover, we observed elevated activity of soluble catalase, a glutathione-independent H_2O_2 scavenging enzyme (47.90 ± 1.47 vs 78.20 ± 7.20, controls vs DM samples, $p < 0.01$) (Table II).

The glutathione-dependent H_2O_2 scavenger, glutathione peroxidase displayed comparable activity between controls and diabetics (18.54 ± 1.26 and 21.70 ± 0.90, n.s.). Moreover, neither glutathione S-transferase, the enzyme that facilitates dissolution of insoluble oxidative agents into aqueous media (26.41 ± 4.78 vs 33.23 ± 4.38, controls vs DM samples, n.s.), nor glutathione reductase (63.57 ± 2.45 vs 56.30 ± 4.00, controls vs DM samples, n.s.) displayed variations in activity between the two groups (Table II).

Intracellular Ca^{2+} homeostasis

To determine whether the Ca^{2+} balance is modified in lymphocytes from diabetic patients in relation to healthy controls, the analysis of intracellular Ca^{2+} levels ($[Ca^{2+}]_i$) and their regulatory mechanisms was performed.

We analyzed the presence of the main Ca^{2+}-specific channels with binding methods using cell-free models (isolate membranes and whole homogenates derived from lymphocytes) (Table III). One of these is comparable to the L-type voltage-dependent Ca^{2+} channel (dihydropyridine receptor channel—DHPR) that controls Ca^{2+} influx from the outside, while two others are receptor-operated, specifically, (i) IP_3-operated Ca^{2+} channels and (ii) Ryanodine receptor (RyR), both involved in mediating Ca^{2+} release from intracellular stores [29]. The presence of L-type Ca^{2+} channels, that play a significant role in Ca^{2+} influx-induced pathways mediating T lymphocyte activation and proliferation [30], are based on the binding of [^{3}H]PN200-110, a selective radioligand for DHPRs. The data disclose a significant increase in [^{3}H]PN200-110-specific binding in lymphocytes of diabetic patients compared with controls (1.169 ± 0.110 vs 0.691 ± 0.003, $p < 0.01$) (Table III).

The capacity values of RyR channels determined using 1 nM ^{3}H-Ryanodine as a specific agonist are presented in Table III, Row 2. Under these conditions, no significant differences were evident between RyR channel receptors of diabetic patients and healthy subjects.

However, the IP_3 depending-Ca^{2+} channel was positively influenced by diabetes compared with

Table II. Oxidative stress status in lymphocytes derived from DM patients, compared to healthy subjects.

	Healthy	DM	*p*
(A) ROS generation			
H_2O_2 generation (μg H_2O_2)	0.99 ± 0.01	1.87 ± 0.03	<0.01
$O_2^{\cdot -}$ formation (O.D. × 100)	72.40 ± 0.60	75.80 ± 0.37	<0.01
(B) Oxidative stress markers			
Lipid peroxidation (nmol/mg prot of Malondialdehyde)	7.83. ± 1.11	12.43 ± 1.44	<0.05
Protein oxidation (nmol/mg prot of DNHP)	3.58 ± 0.24	6.32 ± 0.15	<0.01
(C) Antioxidant enzyme activities			
Catalase (nmol/min/mg prot)	47.90 ± 1.47	78.20 ± 7.20	<0.01
Glutathione S-Transferase (nmol/min/mg prot)	26.41 ± 4.78	33.23 ± 4.38	n.s.
Superoxide dismutase (U/mg prot)	42.50 ± 5.10	97.00 ± 3.80	<0.01
Glutathione peroxidase (nmol/min/mg prot)	18.54 ± 1.26	21.70 ± 0.90	n.s.
Glutathione reductase (nmol/min/mg prot)	63.57 ± 2.45	56.30 ± 4.00	n.s.

Results are expressed as means ± SEM, $n = 5$. Statistical significance was calculated using the Student's *t*-test for unpaired data.
(A) ROS generation: (1) Hydrogen peroxide (H_2O_2) production was assayed using a colourimetric method based on the oxidation of iodide in the presence of ammonium molybdate. Values are expressed as μg H_2O_2 per 10^5 cells; (2) Intracellular $O_2^{\cdot -}$ formation was assessed using the nitroblue tetrazolium reduction assay (see Methods).
(B) Oxidative Stress markers: (1) Oxidative damage derived from lipid peroxidation is expressed as relative values (nmol/mg prot) of Malondialdehyde; (2) Protein oxidative damage was measured as the protein carbonyl content. Values are derived from the reaction between DNPH and protein carbonyl.
(C) Antioxidant enzyme activities: (1) Catalase activity was determined according to the method described by Fanò et al. [16], based on the decrease in absorbance due to H_2O_2 consumption ($\varepsilon = -0.04$ mM^{-1} cm^{-1}) measured at 240 nM; (2) Glutathione S-transferase activity was determined using CDNB as the substrate (see Methods); (3) Superoxide dismutase (SOD) activity was determined using a modified method of L'Abbé and Fischer [18]. SOD units were calculated using the definition of a SOD unit as the activity that inhibits the rate of cytochrome c reduction by 50%; (4) Glutathione reductase activity was measured according to the rate of decrease in absorbance induced by NADPH oxidation at 340 nm; (5) Glutathione peroxidase activity was calculated with the method of Lawrence and Burk [20], which involves the measurement of GSSG formation using a coupled enzyme system with glutathione reductase.

controls (0.370 ± 0.090 vs 0.285 ± 0.032, $p < 0.05$, Table III). Since the increased capacity of Ca^{2+} channels induces a sustained Ca^{2+} flux increase (between external and internal stores), it is possible that the intracellular concentration of the ion is elevated, but only if the Ca^{2+} pump mechanism is not altered or depressed.

Notably, experiments evaluating the activity of Ca^{2+}-ATPase show that active Ca^{2+} transport is significantly decreased in pathological lymphocytes compared with controls (470.00 ± 3.10 vs 548.00 ± 5.60, $p < 0.01$).

To ascertain whether effective alterations in $[Ca^{2+}]_i$ homeostasis occur in lymphocytes derived from DM patients, video-imaging analysis of single cells were performed in the presence of pharmacological or physiological agents that modulate $[Ca^{2+}]_i$. The results show that two populations are present (at least in terms of the basal Ca^{2+} level) in both healthy and diabetic samples, specifically, one with basal levels of 138.0 ± 7.8 nM and 146.2 ± 19.7 nM, respectively, and another with levels of 509.0 ± 19.8 nM in healthy controls and 625.5 ± 46.5 nM ($p < 0.05$) in diabetics (Figure 1).

However, the population percentage with a higher intracellular Ca^{2+} resting level doubled in DM lymphocytes (39% vs 19%).

Spontaneous Ca^{2+} waves are recorded and generated in 19% of DM lymphocyte population (Figure 2).

In the presence of 40 mM KCl, capable of inducing a shift in L-type Ca^{2+} channels to the open status and capacitative Ca^{2+} release from internal stores

Table III. Functional characteristics of Ca^{2+} channels (L-type; IP_3-operated and RyR-specific) and Ca^{2+}-dependent pump activity.

$n = 5$	Healthy	DM	*p*
L-type: ([^{3}H]PN200-110 binding) (pmol/mg prot)	0.691 ± 0.003	1.169 ± 0.110	<0.01
RyR1 [^{3}H]RyR1 binding (pmol/mg prot)	2.627 ± 0.173	2.773 ± 0.202	n.s.
IP_3 binding (pmol/mg prot)	0.285 ± 0.032	0.370 ± 0.09	<0.05
Ca^{2+}-ATPase (P_i μg/min/ml/mg prot)	548.00 ± 5.60	470.00 ± 3.10	< 0.01

Binding experiments to test the functional capacity of different channels to induce Ca^{2+} translocation from external (L-type DHPR Ca^{2+}-channels) and internal stores (Ca^{2+}-operated RyR channel or IP_3-sensitive Ca^{2+} channel). Binding experiments were performed on homogenates derived from both healthy and DM lymphocytes. Data are expressed as means ± SD (see Methods for details).
Ca^{2+}-ATPase activity. The assay was performed on homogenates obtained from sonicated lymphocytes, as described in the Methods section.

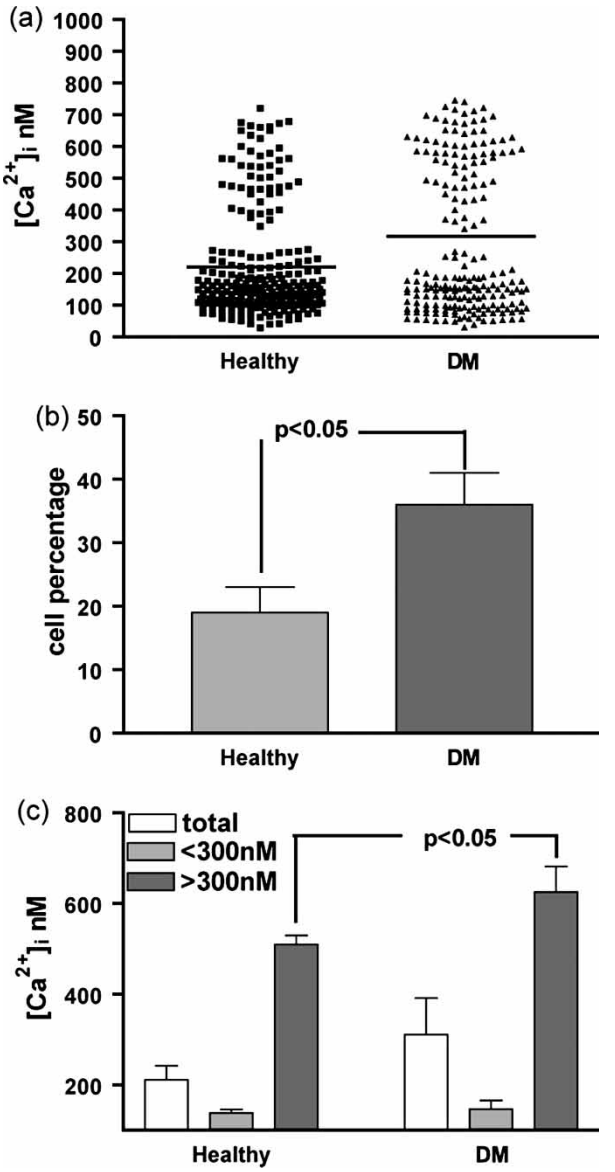

Figure 1. Intracellular Ca^{2+} levels recorded in isolated lymphocytes from healthy controls and DM patients. Measurements were performed by video imaging of single cells plated on poly-L-lysine-coated 12 mM glass coverslips. (A) The basal $[Ca^{2+}]$i values in the tested cells (control: $n=243$; DM: $n=201$). Cell distributions revealed two cell populations: the first with basal $[Ca^{2+}]$i values higher than 300 nM and the latter showing $[Ca^{2+}]$i values lower than 300 nM. (B) The percentage (mean $\pm$SEM) of lymphocytes derived from healthy and DM subjects with resting $[Ca^{2+}]$i values higher than 300 nM. Histograms in (C) represent the mean values ($\pm$SEM) of the basal $[Ca^{2+}]$i measured in lymphocytes derived from considering cell population distributions. Mean values of baselines for healthy subjects were: 211.08 $\pm$ 30.7 considering the whole cell population (total); 138.0 $\pm$ 7.8 nM considering the cell population showing basal $[Ca^{2+}]$i lower than 300 nM ($<$ 300 nM) and 509.0 $\pm$ 19.8 nM for the population with $[Ca^{2+}]$i higher than 300 nM ($>$300 nM), while in the DM patients, the ion concentrations were: 311.02 $\pm$ 80.4; 146.2 $\pm$ 19.7 nM and 625.5 $\pm$ 46.5 nM, respectively.

(Figure 2), we observed at least four different modalities (in both DM and healthy lymphocytes) of cell responses (Figure 3, Panels 1–4).

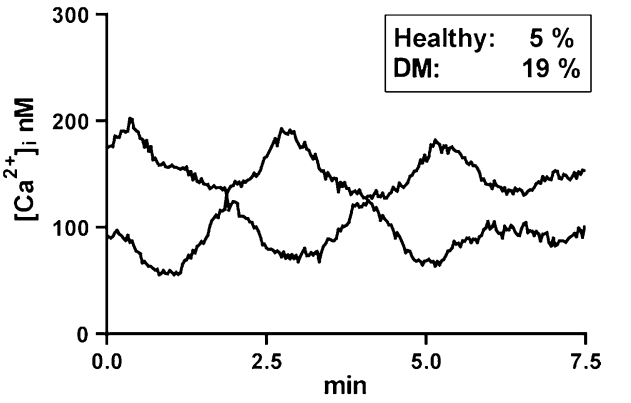

Figure 2. Spontaneous calcium waves in isolated lymphocytes. Measurements were performed as described in Figure 1. The traces represent the spontaneous activity of single cells recorded in lymphocyte population from healthy ($n=115$) or DM subjects ($n=157$). In the box cell percentages showing calcium waves are reported.

One observed kinetic effect was a rapid $[Ca^{2+}]_i$ increase (up to 5-times vs baseline) with a fast uprising and recovery (full activation) (Figure 3, Panel 1). Thapsigargin (Tg), a drug that effectively blocks the Ca^{2+} pumps of endoplasmic membranes and clears the internal stores, only induced a slight and transitory Ca^{2+} increase (Panel 1). About 70% of all tested responsive cells (72 healthy and 69 DM) displayed this time-course. A second trend (slight activation) was significantly observed solely in control lymphocytes (22%), but was almost absent (5%) in cells derived from DM patients (Panel 2). This second time-course is characterized by partial emptying of intracellular stores via a capacitative mechanism, since the addition of 1 μM Tg induced a large and sustained Ca^{2+} increase. In DM lymphocytes, an altered mechanism of capacitative Ca^{2+} increase is evident, at least in a significant part of the population. In fact, the percentage of unresponsive or uncoupled cells is significantly higher in pathological samples (Panels 3 and 4; 10% and 16%, respectively), compared to those from healthy subjects displaying similar behaviour.

Moreover, the capacitative Ca^{2+} increase induced by KCl is almost entirely attributed to ionic release from internal stores, since it is independent of the presence of external Ca^{2+} (Figure 4).

Conversely, no differences exist between the cells of pathological and healthy subjects in terms of RyR-dependent Ca^{2+} increase induced by 40 mM caffeine (data not shown).

Discussion

During the last few decades, the importance of free radicals, highly reactive and deleterious molecules, in human health has progressively been established.

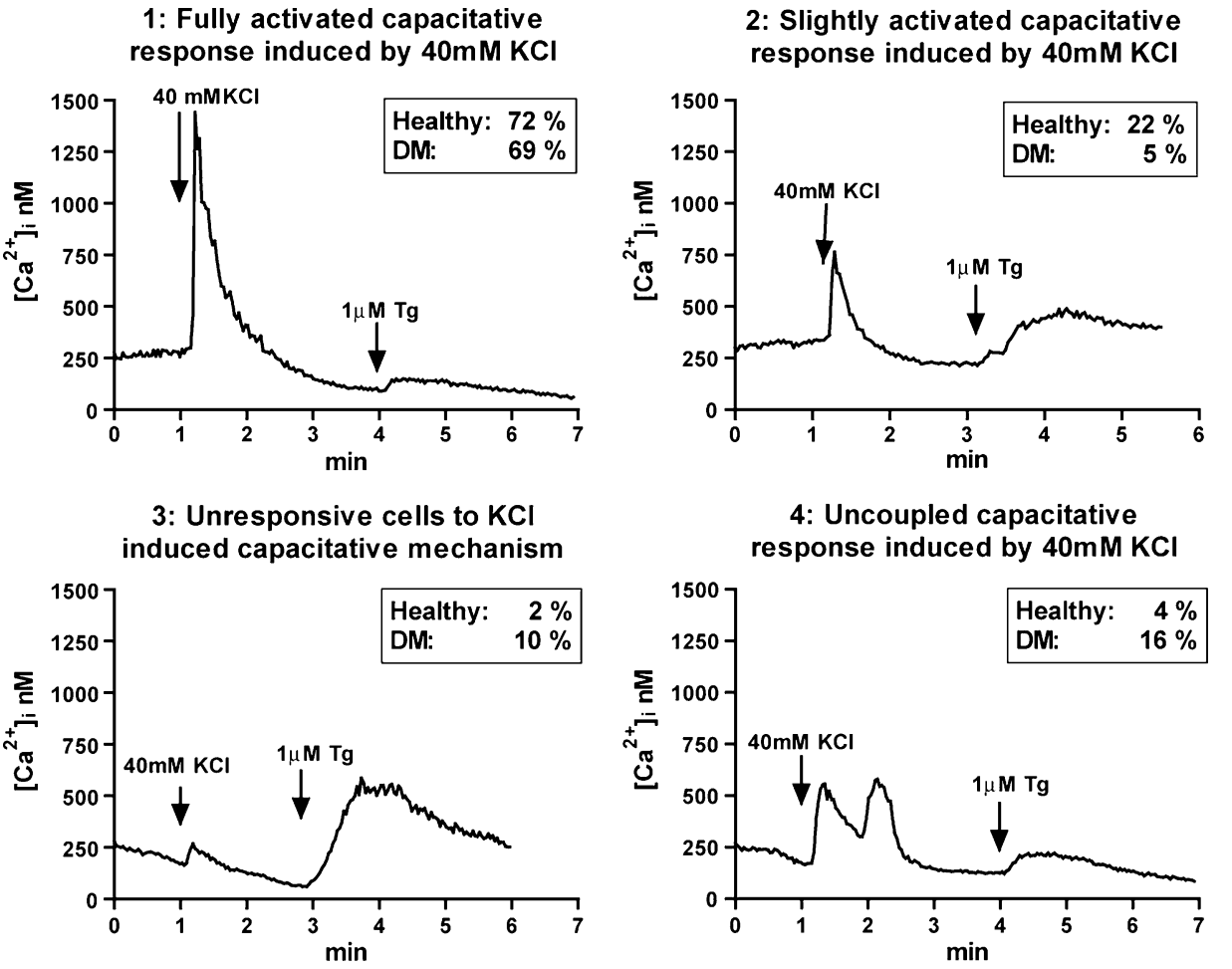

Figure 3. Intracellular Ca^{2+} levels recorded in isolated lymphocytes stimulated with 40 mM KCl. Measurements were performed as described in Figure 1. Panels 1–4 depict intracellular calcium variations ($[Ca^{2+}]$i nM) in cells stimulated with 40 mM KCl. The compound induced different responses: (A) fully activated capacitative calcium increase (Panel 1); (B) slightly activated capacitative calcium increase (Panel 2); (C) no response (Panel 3); (D) uncoupled capacitative response (Panel 4). After the addition of KCl, cells were treated with thapsigargin (1 μM Tg) that elicited differential amplification of cell responses. The trace in each graph represents $[Ca^{2+}]$i variations in a single representative cell, calculated from the recorded single Fluo4-loaded cell fluorescence (see Materials and methods). The box in each graph shows the collective percentage of cells that display a reported kinetic effect in healthy ($n = 137$–157) and DM ($n = 117$–125) cell populations.

Oxygen radicals, reactive non-radical oxygen species, as well as carbon, nitrogen and sulphur radicals have been linked to several human disease conditions, such as atherosclerosis, hypertension, diabetes and cancer [31]. Oxidative stress occurs when the balance between ROS production and the ability of cells or tissues to detoxify free radicals generated during metabolic activity is directed in favour of the former. In particular, for type 2 diabetes, accumulating evidence supports the hypothesis that hyperglycemia results in ROS generation, finally leading to increased oxidative stress in a variety of tissues [32]. Other possible sources of ROS in diabetes include enzymatic pathways, auto-oxidation of glucose and mitochondrial superoxide production [33]. One consequence of ROS imbalance is the expression of gene products that cause cellular damage and major complications in diabetes. Oxidative stress plays a recognized role in cellular signalling involving cytosolic Ca^{2+} and is strictly related to the elevated cytosolic Ca^{2+} concentration due to an imbalance in homeostasis [6]. However, in lymphocytes, ROS may also represent cellular effectors capable of transducing receptor-mediated Ca^{2+} signals [34].

Using peripheral lymphocytes from type 2 diabetes mellitus patients, we analysed the relationship between intracellular Ca^{2+} homeostasis and the oxidative status, particularly with respect to: (i) ROS accumulation, (ii) oxidative damage and (iii) alterations in Ca^{2+} homeostasis.

Our results reveal that lymphocytes from diabetic patients contain significantly higher intracellular H_2O_2 levels, compared to those from healthy subjects. Elevated levels were observed, despite increased activity of the GSH-independent antioxidant pathway (Catalase) that was unable to counteract the accumulation of H_2O_2, the main source of ROS in this setting [2]. H_2O_2, in turn, induces $O_2^{\cdot -}$ production

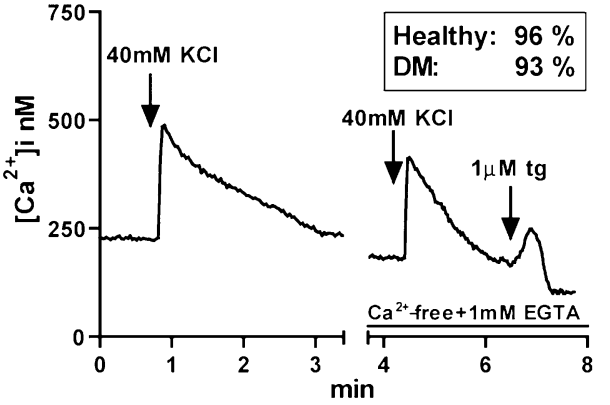

Figure 4. Capacitative response to 40 mM KCl in external Ca^{2+}-free medium. The trace represents the capacitative response to 40 mM KCl in the absence of extracellular calcium (Ca^{2+}-free+EGTA). The trace is calculated from the recorded single Fluo4-loaded cell fluorescence (see Materials and methods). The box in the graph shows the collective percentage of cells that display a reported kinetic effect in healthy ($n=145$) and DM ($n=131$) cell populations.

by activating NADPH oxidase [35]. Moreover, under these conditions, SOD activity to attenuate $O_2^{\cdot -}$ accumulation is increased. However, the effects of ROS accumulation in DM lymphocytes are clearly evident from protein oxidative damage (increased formation of protein carbonyls) and elevated peroxidation of membrane lipids. Despite the wealth of evidence supporting the existence of oxidative stress in DM lymphocytes [2], no conclusive data are available on the cellular targets and/or mechanisms triggered by the antioxidant burden.

Previous reports suggest that the elevated cytosolic calcium concentration in diabetic lymphocytes affects cellular functions [36,37]. Calcium ions play a critical role in the activation of immune cells [29] and increasing intracellular concentrations represent a pivotal event in the control of signal transduction pathways inducing apoptosis and/or necrosis via NF-kB activation [38]. The Ca^{2+} concentration in immune cells is regulated by the calcium-induced calcium release (CICR) mechanism, depending on the trans-plasmamembrane (i.e. voltage-dependent channels) Ca^{2+} influx, followed by sustained release through store-operated Ca^{2+} channels [39]. While IP_3-mediated Ca^{2+} release is a key messenger in the regulation of intracellular Ca^{2+} concentrations through this mechanism, recent studies hypothesize that other receptor-operated channels, i.e. the RyR, contribute to Ca^{2+} signalling in immune cells [39,40]. RyR was initially identified in the sarcoplasmic reticulum of skeletal muscle (RyR_1 type) [41] and cardiac muscle (RyR_2 type) [42]. Hosoi et al. [29] showed that human B cells express RyR equivalent to skeletal muscle type 1. Expression of RyR has additionally been reported in human Jurkat [29] and murine T lymphoma cells [43].

Moreover, while lymphocytes are not classified as 'excitable' cells, there is evidence for the existence of voltage-dependent-like Ca^{2+} channels in the plasmamembranes of T lymphocytes [30]. These Ca^{2+} channels, which share common structural features with excitable cells, may represent 'voltage-operable' channels with different electrophysiological properties [44]. However, the modulatory activity of dihydropyridine, a pharmacological agonist for the common L-type voltage-dependent Ca^{2+} channel, suggests that these channels are involved in the calcium response of these cells [44].

In blood cells, activation of Ca^{2+} entry from the extracellular medium is driven by depletion of endoplasmic reticulum Ca^{2+} stores and occurs through specialized plasmamembrane channels named Ca^{2+}-release-activated Ca^{2+} (CRAC) channels [45]. In lymphocytes, capacitative calcium entry induces the mitogenic response to receptor activation and is thus essential for short-term receptor-controlled cellular responses, such as secretion and chemotaxis. Capacitative calcium entry is additionally involved in longer-term cellular control mechanisms that support T- and B-cell growth, differentiation and death via changes in gene transcription [44,46,47].

An oxidative status able to induce consistent alterations in lipids and proteins [48] may modify mechanisms, such as capacitative Ca^{2+} entry, depending on the presence of adequate structural and functional supports, such as ionic channels and active transport pumps.

When modified protein substrates or peroxidated lipids are correlated with alterations in the intracellular Ca^{2+} equilibrium, specific changes are usually detected at the level of ionic channels and/or transport systems, leading to abnormal cellular activity [49]. Our experiments clearly show that DM-enhanced oxidative stress, which is mainly correlated with H_2O_2 accumulation, induces significant modifications in both external membrane L-type and IP_3-operated Ca^{2+}-channels. These alterations possibly trigger an increase in the Ca^{2+} flux, in turn enhancing the intracellular Ca^{2+} concentration. Since the Ca^{2+} pump activity is concomitantly depressed, the hypothesis that intracellular Ca^{2+} accumulates is feasible. This theory is consistent with data obtained from video-imaging experiments on DM lymphocytes, which show that DM samples have a higher percentage of cells with a basal intracellular Ca^{2+} concentration >300 nM than that in controls and more cells display (directly or indirectly) alterations in mechanisms connected with CRAC.

In conclusion, our data collectively confirm a close relationship between oxidative stress in lymphocytes derived from DM patients and imbalance in intracellular Ca^{2+} homeostasis. The deleterious effects, which occur mainly as a result of accumulation of

H_2O_2 and to a lesser extent, $O_2^{\bullet -}$, despite a significant increase in Catalase and SOD activities, lead to drastic modifications in the capacitative Ca^{2+} transport mechanism and consequently the short- and long-term processes regulated by this ion.

Acknowledgements

This work was supported by Universita' G. d'Annunzio research grants to MAM, GF and GD.

***Declaration of interest*:** The authors report no conflicts of interest. The authors alone are responsible for the content and writing of the paper.

References

[1] Davi G, Falco A, Patrono C. Lipid peroxidation in diabetes mellitus. Antioxid Redox Signal 2005;7:256–268.
[2] West IC. Radicals and oxidative stress in diabetes. Diabet Med 2000;17:171–180.
[3] Reznick AZ, Packer L. Oxidative damage to proteins: spectrophotometric method for carbonyl assay. Methods Enzymol 1994;233:357–363.
[4] Selvaraj N, Bobby Z, Sridhar MG. Oxidative stress: does it play a role in the genesis of early glycated proteins? Med Hypotheses 2008;70:265–268.
[5] Pop-Busui R, Sima A, Stevens M. Diabetic neuropathy and oxidative stress. Diabetes Metab Res Rev 2006;22:257–273.
[6] Camello-Almaraz C, Gomez-Pinilla PJ, Pozo MJ, Camello PJ. Mitochondrial reactive oxygen species and Ca2+ signaling. Am J Physiol Cell Physiol 2006;291:C1082–C1088.
[7] Davi G, Chiarelli F, Santilli F, Pomilio M, Vigneri S, Falco A, Basili S, Ciabattoni G, Patrono C. Enhanced lipid peroxidation and platelet activation in the early phase of type 1 diabetes mellitus: role of interleukin-6 and disease duration. Circulation 2003;107:3199–3203.
[8] Davi G, Ciabattoni G, Consoli A, Mezzetti A, Falco A, Santarone S, Pennese E, Vitacolonna E, Bucciarelli T, Costantini F, Capani F, Patrono C. *In vivo* formation of 8-iso-prostaglandin f2alpha and platelet activation in diabetes mellitus: effects of improved metabolic control and vitamin E supplementation. Circulation 1999;99:224–229.
[9] Levy J. Abnormal cell calcium homeostasis in type 2 diabetes mellitus: a new look on old disease. Endocrine 1999;10:1–6.
[10] Vincent AM, Russell JW, Low P, Feldman EL. Oxidative stress in the pathogenesis of diabetic neuropathy. Endocr Rev 2004;25:612–628.
[11] Boyum A. Isolation of lymphocytes, granulocytes and macrophages. Scand J Immunol 1976;(Suppl 5):9–15.
[12] M'Bemba-Meka P, Lemieux N, Chakrabarti SK. Role of oxidative stress, mitochondrial membrane potential, and calcium homeostasis in nickel sulfate-induced human lymphocyte death *in vitro*. Chem Biol Interact 2005;156:69–80.
[13] Rauen U, Petrat F, Li T, De Groot H. Hypothermia injury/cold-induced apoptosis--evidence of an increase in chelatable iron causing oxidative injury in spite of low O_2-/H_2O_2 formation. Faseb J 2000;14:1953–1964.
[14] Fulle S, Mecocci P, Fano G, Vecchiet I, Vecchini A, Racciotti D, Cherubini A, Pizzigallo E, Vecchiet L, Senin U, Beal MF. Specific oxidative alterations in vastus lateralis muscle of patients with the diagnosis of chronic fatigue syndrome. Free Radic Biol Med 2000;29:1252–1259.
[15] Lowry OH, Rosebrough NJ, Farr AL, Randall RJ. Protein measurement with the Folin phenol reagent. J Biol Chem 1951;193:265–275.
[16] Fano G, Mecocci P, Vecchiet J, Belia S, Fulle S, Polidori MC, Felzani G, Senin U, Vecchiet L, Beal MF. Age and sex influence on oxidative damage and functional status in human skeletal muscle. J Muscle Res Cell Motil 2001;22:345–351.
[17] Habig WH, Jakoby WB. Assays for differentiation of glutathione S-transferases. Methods Enzymol 1981;77:398–405.
[18] L'Abbe MR, Fischer PW. An automated method for the determination of Cu,Zn-superoxide dismutase in plasma and erythrocytes using an ABA-200 discrete analyzer. Clin Biochem 1986;19:175–178.
[19] Ramos-Martinez JI, Bartolome TR, Pernas RV. Purification and properties of glutathione reductase from hepatopancreas of mytilus edulis M. Comp Biochem Physiol 1983;75B:689–692.
[20] Lawrence RA, Burk RF. Glutathione peroxidase activity in selenium-deficient rat liver. Biochem Biophys Res Commun 1976;71:952–958.
[21] Fulle S, Di Donna S, Puglielli C, Pietrangelo T, Beccafico S, Bellomo R, Protasi F, Fano G. Age-dependent imbalance of the antioxidative system in human satellite cells. Exp Gerontol 2005;40:189–197.
[22] Fulle S, Belia S, Vecchiet J, Morabito C, Vecchiet L, Fano G. Modification of the functional capacity of sarcoplasmic reticulum membranes in patients suffering from chronic fatigue syndrome. Neuromusc Disord 2003;13:479–484.
[23] Treves S, Scutari E, Robert M, Groh S, Ottolia M, Prestipino G, Ronjat M, Zorzato F. Interaction of S100A1 with the Ca2+ release channel (ryanodine receptor) of skeletal muscle. Biochemistry 1997;36:11496–11503.
[24] Mesonero JE, Tanfin Z, Hilly M, Colosetti P, Mauger JP, Harbon S. Differential expression of inositol 1,4,5-trisphosphate receptor types 1, 2, and 3 in rat myometrium and endometrium during gestation. Biol Reprod 2000;63:532–537.
[25] Belia S, Pietrangelo T, Fulle S, Menchetti G, Cecchini E, Felaco M, Vecchiet J, Fano G. Sodium nitroprusside, a NO donor, modifies Ca2+ transport and mechanical properties in frog skeletal muscle. J Muscle Res Cell Motil 1998;19:865–876.
[26] Taussky HH, Shorr E. A microcolorimetric method for the determination of inorganic phosphorus. J Biol Chem 1953;202:675–685.
[27] Guarnieri S, Fano G, Rathbone MP, Mariggio MA. Cooperation in signal transduction of extracellular guanosine 5' triphosphate and nerve growth factor in neuronal differentiation of PC12 cells. Neuroscience 2004;128:697–712.
[28] Ritter M, Menon S, Zhao L, Xu S, Shelby J, Barry WH. Functional importance and caffeine sensitivity of ryanodine receptors in primary lymphocytes. Int Immunopharmacol 2001;1:339–347.
[29] Hosoi E, Nishizaki C, Gallagher KL, Wyre HW, Matsuo Y, Sei Y. Expression of the ryanodine receptor isoforms in immune cells. J Immunol 2001;167:4887–4894.
[30] Kotturi MF, Hunt SV, Jefferies WA. Roles of CRAC and Cav-like channels in T cells: more than one gatekeeper? Trends Pharmacol Sci 2006;27:360–367.
[31] Madamanchi NR, Vendrov A, Runge MS. Oxidative stress and vascular disease. Arterioscler Thromb Vasc Biol 2005;25:29–38.
[32] Lee AY, Chung SS. Contributions of polyol pathway to oxidative stress in diabetic cataract. Faseb J 1999;13:23–30.
[33] Chinopoulos C, Adam-Vizi V. Calcium, mitochondria and oxidative stress in neuronal pathology. Novel aspects of an enduring theme. Febs J 2006;273:433–450.
[34] Hawkins BJ, Solt LA, Chowdhury I, Kazi AS, Abid MR, Aird WC, May MJ, Foskett JK, Madesh M. G protein-coupled receptor Ca2+-linked mitochondrial reactive oxygen species are essential for endothelial/leukocyte adherence. Mol Cell Biol 2007;27:7582–7593.

[35] Matteucci E, Giampietro O. Flow cytometry study of leukocyte function: analytical comparison of methods and their applicability to clinical research. Curr Med Chem 2008;15:596–603.
[36] Alexiewicz JM, Kumar D, Smogorzewski M, Massry SG. Elevated cytosolic calcium and impaired proliferation of B lymphocytes in type II diabetes mellitus. Am J Kidney Dis 1997;30:98–104.
[37] Balasubramanyam M, Premanand C, Mohan V. The lymphocyte as a cellular model to study insights into the pathophysiology of diabetes and its complications. Ann N Y Acad Sci 2002;958:399–402.
[38] Dolmetsch RE, Lewis RS, Goodnow CC, Healy JI. Differential activation of transcription factors induced by Ca2+ response amplitude and duration. Nature 1997;386:855–858.
[39] Zweifach A, Lewis RS. Mitogen-regulated Ca2+ current of T lymphocytes is activated by depletion of intracellular Ca2+ stores. Proc Natl Acad Sci USA 1993;90:6295–6299.
[40] Guse AH, da Silva CP, Berg I, Skapenko AL, Weber K, Heyer P, Hohenegger M, Ashamu GA, Schulze-Koops H, Potter BV, Mayr GW. Regulation of calcium signalling in T lymphocytes by the second messenger cyclic ADP-ribose. Nature 1999;398:70–73.
[41] Sei Y, Gallagher KL, Basile AS. Skeletal muscle type ryanodine receptor is involved in calcium signaling in human B lymphocytes. J Biol Chem 1999;274:5995–6002.
[42] Otsu K, Willard HF, Khanna VK, Zorzato F, Green NM, MacLennan DH. Molecular cloning of cDNA encoding the Ca2+ release channel (ryanodine receptor) of rabbit cardiac muscle sarcoplasmic reticulum. J Biol Chem 1990;265: 13472–13483.
[43] Bourguignon LY, Chu A, Jin H, Brandt NR. Ryanodine receptor-ankyrin interaction regulates internal Ca2+ release in mouse T-lymphoma cells. J Biol Chem 1995;270:17917–17922.
[44] Gomes B, Savignac M, Moreau M, Leclerc C, Lory P, Guery JC, Pelletier L. Lymphocyte calcium signaling involves dihydropyridine-sensitive L-type calcium channels: facts and controversies. Crit Rev Immunol 2004;24:425–447.
[45] Densmore JJ, Haverstick DM, Szabo G, Gray LS. A voltage-operable current is involved in Ca2+ entry in human lymphocytes whereas ICRAC has no apparent role. Am J Physiol 1996;271:C1494–C1503.
[46] Gwack Y, Feske S, Srikanth S, Hogan PG, Rao A. Signalling to transcription: store-operated Ca2+ entry and NFAT activation in lymphocytes. Cell Calcium 2007;42:145–156.
[47] Hakamata Y, Nishimura S, Nakai J, Nakashima Y, Kita T, Imoto K. Involvement of the brain type of ryanodine receptor in T-cell proliferation. FEBS Lett 1994;352:206–210.
[48] De Cristofaro R, Rocca B, Vitacolonna E, Falco A, Marchesani P, Ciabattoni G, Landolfi R, Patrono C, Davi G. Lipid and protein oxidation contribute to a prothrombotic state in patients with type 2 diabetes mellitus. J Thromb Haemost 2003;1:250–256.
[49] Putney JW Jr. New molecular players in capacitative Ca2+ entry. J Cell Sci 2007;120:1959–1965.

This paper was first published online on iFirst on 27 December 2008.